Authorized Reprint from
Special Technical Publication 570

American Society for Testing and Materials
1916 Race Street, Philadelphia, Pa. 19103
1976

G. L. Kulcinski,[1] *D. G. Doran,*[2] *and M. A. Abdou*[3]

Comparison of Displacement and Gas Production Rates in Current Fission and Future Fusion Reactors

REFERENCE: Kulcinski, G. L., Doran, D. G., and Abdou, M. A., **"Comparison of Displacement and Gas Production Rates in Current Fission and Future Fusion Reactors,"** *Properties of Reactor Structural Alloys After Neutron or Particle Irradiation, ASTM STP 570,* American Society for Testing and Materials, 1975, pp. 329–351.

ABSTRACT: The displacement, helium production, and hydrogen production rates in five candidate materials for controlled thermonuclear reactors (CTR) (Type 316 stainless steel, molybdenum, columbium, vanadium, and sintered aluminum product) were calculated for seven potential irradiation facilities. The damage rates were calculated for two fast fission reactors (fast flux test facility and Experimental Breeder Reactor-II), two thermal reactors (high flux isotope reactor and experimental test reactor), two accelerator neutron sources (Los Alamos Meson Production Facility and rotating target neutron source), and a typical CTR blanket. It was found that while fission reactors can easily duplicate displacement damage rates typical of CTR first walls, they fall short, sometimes by several orders of magnitude, of duplicating the helium and hydrogen production rates. The one exception to the latter statement is that helium production in stainless steel, due to the ^{59}Ni production, can even be higher in thermal fission reactors than in CTR. Accelerator sources produce damage which is more like that in CTR, but the absolute magnitude in current facilities is too low by at least an order of magnitude. It is concluded that the high flux isotope reactor is currently the best neutron facility to simulate fusion reactor damage.

KEY WORDS: radiation, irradiation, power reactors (nuclear), displacement, simulation, helium, hydrogen

[1] Professor, Nuclear Engineering Department, University of Wisconsin, Madison, Wis. 53706.
[2] Senior research scientist, Hanford Engineering Development Laboratory, Richland, Wash. 99352.
[3] Research scientist, Argonne National Laboratory, Argonne, Ill. 60439.

The structural components of controlled thermonuclear fusion reactor (CTR) blankets will be subjected to the most severe high temperature irradiation environment that has even been imposed on solid materials [*1–5*].[4] The safe and economical operation of CTR will, to a large degree, depend on how successful scientists are in choosing metals and alloys that can retain adequate strength, ductility, and dimensional stability under such conditions. These mechanical and physical properties are very sensitive to the total number of times each atom is displaced in a solid during the component's lifetime [*6–9*]. Previous estimates [*1–5*] predicted that the atoms in CTR blanket components will theoretically be displaced up to several hundred times per year at temperatures of 500 to 1000°C. These displaced atoms and their vacant lattice sites are known to precipitate into clusters that can cause significant volume changes [*6–8*]. Another factor that has been shown to greatly effect the mechanical properties of metals irradiated in fission reactors is the amount of neutronically generated gases present in metal. These gases come from (n,α), $(n,n'\alpha)$, (n,p), $(n,n'p)$, (n,d), and (n,t) reactions characteristic of high energy neutrons. The cross sections for such reactions are usually appreciable only above a few million electron volts in most elements. Whereas it has already been found that helium concentrations typical of fission reactor environments (~1 to 10 atomic parts per million (appm)) can cause high temperature embrittlement [*9–11*], the situation is expected to be much worse for CTR because the transmutation cross sections for the 14 MeV neutrons are much higher.

It is obvious that if we ever expect to construct large scale CTR, we must know the quantitative values of the displacement and transmutation rates in potential CTR materials. Since high power fusion reactors will not be available until the late 1980's [*12*], we must also attempt to simulate those conditions as best we can in current irradiation facilities and test the components under typical CTR conditions to see if they will meet the design requirements.

The main purpose of this paper is to show what range of displacement and transmutation rates we might expect in fusion reactors for materials such as columbium, vanadium, molybdenum, aluminum, or stainless steel, which are currently being considered for CTR applications. We will also address the question of what current facilities (fast and thermal reactors as well as 14-MeV accelerator neutron sources) might be used to simulate the calculated damage rates.

We will limit our discussion to our current concept of how a CTR blanket might look some 20 years from now. Therefore, we have chosen a blanket similar to that designed by the University of Wisconsin Fusion Reactor

[4] The italic numbers in brackets refer to the list of references appended to this paper.

Study Group [*13*]. It is felt that this blanket is a reasonable structure to accomplish the neutron slowing down, energy removal, and breeding objectives of a CTR. We recognize that the ultimate blanket design will be much more detailed and perhaps somewhat different in its size, shape, and placement of major components.

Description of Calculational Procedures

Blanket Design

The CTR blanket design chosen for this study is similar to that used for a 5000 MW(th) Tokamak reactor study [*13*]. The details of the structure have been homogenized in a manner better suited for neutronics calculations. There are basicially five regions to consider: a 1-cm-thick first wall; a 42-cm-thick breeding and cooling zone which is 95 percent natural lithium and 5 percent structural material; a 20-cm-thick stainless steel reflector; a 7-cm-thick cooling region again composed of 95Li and 5 percent structure; and a 1-m-thick shield composed of 70Pb and 30 percent boron carbide.

Flux Spectra

The neutron spectra in the various blankets have been calculated by substituting the various metals into the fusion blanket described previously and using the discrete ordinate program ANISN [*14*]. All calculations were made in one-dimensional cylindrical geometry using the P_3–S_6 approximations. Neutron cross section data has been obtained from Evaluated Nuclear Data File, (ENDF/B-III) [*15*] and processed by the MACK [*16*] code into either a 100 or 46 energy group structure ranging from 0.022 eV to 14.918 MeV. The 14-MeV neutron source to the first wall was normalized to 1 MW/m^2 (4.43×10^{13} neutrons (n)/cm^2/s) so that all CTR results are reported per unit of neutron wall loading.

The same volume of metal was used in each fusion blanket calculation although in practice the amount may vary with the specific material (for example, less molybdenum may be needed than aluminum). However, since the spectra in a fusion reactor are primarily determined by the lithium, the exact amount of structural material has very little effect on the neutron spectra. It should be noted that it is not practical to consider pure aluminum as a wall material because of its low strength at high temperature. Therefore, we have used sintered aluminum product (SAP) as a realistic substitute; SAP is simply high purity aluminum which is strengthened by the addition of 5 to 10 percent by weight of aluminum oxide in the form of very fine particles in the matrix. Some characteristics of this material for CTR application have recently been described by Powell et al [*17*].

The neutron flux spectra for two fast reactors, Experimental Breeder

Reactor-II (EBR-II) and fast flux test facility (FFTF), were obtained.[5] The core center, row two spectra at 62.5 MW(th) as unfolded by SAND-II was used for Experimental Breeder Reactor-II (EBR-II) and the core center driver fuel assembly spectrum was used for FFTF. Data from two current thermal test reactors, experimental test reactor (ETR) and high flux isotope reactor (HFIR) [*18*], were also used. The target spectrum in HFIR, PTP location, was used for 100-MW operation and the midplane data for row L-8 unfolded by SAND-II were used for ETR operating at 175 MW.

The neutron spectra for the Los Alamos Meson Production Facility (LAMPF) were obtained from Dudziak and Sherman [*19*] for a 0.5-mA beam of 800-MeV protons on a water cooled copper target with a nickel reflector. The total flux at the specimen was calculated to be 2×10^{14} n/cm^2/s of which only 3.6 percent was above 10 MeV and 1.45 percent in the 10 to 25-MeV interval.

The rotating target neutron source (RTNS) at Lawrence Livermore Laboratory [*20*] currently has a 14-MeV current of $\sim 2 \times 10^{12}$ n/cm^2/s. At the present time, there is no provision for surrounding specimens with CTR type blankets to take advantage of backscattered neutrons, although such a facility would be relatively easy to build. Therefore, we have assumed the theoretical displacement and gas production rates in the RTNS would be similar to those in a CTR first wall but scaled down to a 0.045 MW/m^2 wall loading.

Displacement Cross Sections

Neutron interactions with nuclei that are treated explicitly in this work include elastic scattering, inelastic scattering, $(n,2n)$ and (n,γ). Charged particle reactions are neglected for all metals but aluminum. This introduces no more than a 5 percent error in the displacement cross sections of the refractory metals and 15 percent in stainless steel at 15 MeV. The error decreases rapidly with decreasing energy. In the case of aluminum, (n,α) and (n,p) reactions are included in an approximate manner by adding the cross sections to the inelastic scattering cross section. This is to take account of the kinetic energy given the emitting nucleus. The damage produced by the emitted proton or alpha particle is negligible; for example, the number of displacements produced by the alpha particle in the $^{27}\mathrm{Al}(n,\alpha)^{24}\mathrm{Ni}$ reaction was calculated to be < 1 percent of that produced by the nucleus. The charged particle reactions add ~ 30 percent to the displacement cross section of aluminum at 15 MeV.

It should be pointed out that charged particle reactions, including (n,np), dominate the displacement cross section of nickel at 15 MeV and should be taken into account in any consideration of high nickel content alloys.

[5] Obtained from Dosimetry Center, Hanford Engineering Development Laboratory.

The mechanisms listed above produce primary knock-on atoms (PKA) which in turn lose their energy by electronic excitation or nuclear energy transfers to surrounding atoms. This latter form of energy transfer causes further displacements. The total displacement cross section at energy, E, is just

$$F(E) = F_{el}(E) + F_{inel}(E) + F_{(n,2n)}(E) + F_{(n,\gamma)}(E) \tag{1}$$

where

$F_{el}(E)$ = displacement cross section due to both isotropic scattering at low energies (< 0.1 MeV) and anisotropic scattering at higher energies,
$F_{inel}(E)$ = displacement cross section due to (n,n') scattering,
$F_{(n,2n)}(E)$ = displacement cross section due to $(n,2n)$ reactions, and
$F_{(n,\gamma)}(E)$ = displacement cross section due to the energetic recoils which result from (n,γ) reaction (mainly from low energy neutrons).

The general expression for $F(E)$ is

$$F(E) = \sigma(E) \int_{E_d}^{T_{max}} p(\bar{E},T)\, \nu(T) dT \tag{2}$$

where

$\sigma(E)$ = appropriate interaction cross section,
$p(E,T)$ = probability that a neutron of energy, E, transfers T to the PKA,
$\nu(T)$ = number of displacements produced by a PKA with energy T, and
E_d = minimum energy required to displace an atom.

The problem then boils down to a determination of the number and energy spectrum of the PKA from $\sigma(E)$ and $p(E,T)$, and the choice of a model to calculate the average number of atoms displaced by each PKA of energy T. The evaluation of $\nu(T)$ is essentially independent of the type of scattering that produced the PKA, and we will consider this problem first.

The results for this study are based on the Lindhard [*21*] theory of slowing down of energetic atoms in solids. Lindhard has derived, from Thomas-Fermi theory, a function, $L(\epsilon)$, which is the kinetic energy (in dimensionless form) that is transferred to the atoms of a cascade initiated by a PKA having initial dimensionless energy, ϵ. That is, the fraction of PKA energy available to cause displacements in $L(\epsilon)/\epsilon$; the remainder is lost in electron excitation. In the present work, the number of displace-

ments per PKA is calculated to be

$$\nu(T) = \beta \frac{L(\epsilon)}{\epsilon} \quad \frac{T}{2E_d} \tag{3}$$

where

E_d = effective displacement energy,
$\epsilon = A_L T$ and for pure materials of atomic number Z and atomic weight A,

$$A_L = \frac{0.01151}{(Z)^{7/3}} \text{ eV}^{-1}, \text{ and}$$

$$L(\epsilon) = \frac{\epsilon}{[1 + K_L g(\epsilon)]} \text{ (see Ref 22)},$$

where

$$g(\epsilon) = \epsilon + 0.40244\epsilon^{3/4} + 3.4008\epsilon^{1/6},$$

$$K_L = \frac{0.1334(Z)^{2/3}}{A^{1/2}}, \text{ and}$$

$$\beta \cong 0.8$$

Beta is a numerical factor to account for the deviation from a hard sphere potential during a two body collision [23].

It should be noted that $\nu(T)$ is very sensitive to the choice of E_d. There is considerable controversy over what one should use for this number: the threshold energy required to displace an atom in the easiest direction or the maximum energy required to displace an atom in the close packed direction or some arbitrary combination of all these values. Because of this uncertainty, we have chosen to report the displacement cross section in terms of barns and electron volts which will allow each investigator to choose his own value of E_d.

It has recently been suggested that the effective displacement energy in iron might be taken as 1.67 times the threshold value [23]. For lack of a more definite model at this time, we will use the same factor to multiply the threshold displacement energies of the materials considered here. The threshold energies used were 36 eV for columbium [24], 37 eV for molybdenum [25], 24 eV for iron [25], and 16 eV for aluminum [26]. We

have arbitrarily chosen the threshold displacement energy as 24 eV for vanadium in keeping with body-centered cubic iron.[6]

The calculation of the PKA energy spectrum is rather straightforward in principle for elastic scattering and (n,γ) reactions but somewhat more complex for inelastic scattering and $(n,2n)$ reactions. It is not the purpose of this paper to discuss the latter two scattering processes in detail as that is covered elsewhere [*27–29*].

The principal source of cross-section data for all metals but iron was ENDF/B-III [*15*]. In the case of iron, MAT-1124 data from ENDF were used. This evaluation differs insignificantly for the present application from the MAT-1180 evaluation included in ENDF/B-III. Some smoothing in the resonance region was carried out for vanadium, molybdenum, chromium, and nickel; and some angular distribution data for chromium and molybdenum were taken from the third election of Brookhaven National Laboratory (BNL-400).

The values of $F(E)$ used for this work are given in Table 1 where the cross sections are multiplied by displacement energies to give the unit of barns and electron volts. Displacement cross sections corresponding to different values of E_d than used here can be obtained by dividing the values in Table 1 by the preferred values of E_d. It should be realized, however, that this procedure is inaccurate when applied to the elastic scattering of neutrons in the few hundred to few thousand electron volt range. This is because the corresponding PKA energies are not sufficiently greater than E_d that the lower limit of the integral of Eq 2 can be taken as zero. Hence, the displacement cross section is not strictly inversely proportional to E_d in this range.

Gas Production Cross Sections

The gas production cross sections for columbium, vanadium, aluminum, oxygen, and Type 316 stainless steel were obtained from ENDF/B-III and averaged over the energy group structure used for the ANISN calculations by the MACK code [*16*]. Cross sections for molybdenum were calculated using Pearlstein's model [*31*]. All the cross sections were assumed to be constant above 15 MeV for the LAMPF calculations following Dudziak [*19*]. No impurity (for example, carbon, nitrogen, silicon, etc.) reactions were considered but the ^{58}Ni(n,γ) ^{59}Ni(n,α) ^{55}Fe reactions were considered in Type 316 stainless steel. The cross sections of Kirouac [*32*] were used for the ^{59}Ni reactions. Figure 1 shows how the (n,α) cross sections vary over the 0 to 15 MeV range (the (n,p) cross sections have the same qualitative shapes). The curves in these figures do *not* include the $(n,n'\alpha)$ contributions

[6] The displacement energy of vanadium has been recently measured to be 26 eV (see Miller, M. G. and Chaplin, R. L., *Radiation Effects*, Vol. 22, 1974, p. 107.

TABLE 1—*Displacement functions for potential CTR materials.*[a]

Lower Neutron Energy, MeV	barn − eV				
	Type 316 Stainless Steel	Mo	Cb	V	Al
13.50[b]	89 000	108 000	103 000	91 400	51 300
12.21	83 100	103 000	96 800	86 900	50 900
11.05	79 700	96 000	91 100	84 000	50 200
10.00	78 200	90 100	86 100	82 300	48 600
9.048	76 500	84 000	82 300	80 500	46 200
8.187	76 100	79 000	78 300	79 000	45 600
7.408	75 900	77 300	74 300	77 600	45 600
6.703	73 900	71 300	69 900	76 100	45 200
6.065	70 500	68 300	65 200	74 500	41 800
5.488	68 100	64 600	60 600	72 800	45 400
4.966	66 400	59 500	56 100	70 200	44 200
4.493	64 900	56 500	51 800	67 800	43 200
4.066	62 400	54 700	47 800	65 200	41 300
3.679	59 700	52 000	44 200	60 300	41 800
3.329	56 400	48 100	41 000	59 000	41 000
3.012	55 000	46 800	38 200	55 700	40 000
2.725	51 800	45 700	36 600	54 500	39 300
2.466	51 000	43 900	36 600	50 100	41 500
2.231	46 700	41 700	35 900	44 900	35 400
2.019	42 000	39 500	34 200	40 200	40 300
1.827	39 900	37 400	32 700	41 500	35 400
1.653	33 000	35 300	31 400	39 700	34 100
1.496	31 600	33 100	30 000	38 800	32 500
1.353	30 300	30 700	28 900	37 200	30 600
1.225	29 100	28 600	28 500	34 800	28 300
1.108	26 000	27 300	27 900	33 200	32 880
1.003	20 700	26 200	27 100	30 600	24 500
0.9072	18 300	24 200	26 400	27 100	22 900
0.8208	17 400	23 300	25 600	26 700	28 800
0.7427	20 400	22 700	25 000	19 300	31 500
0.674	19 600	22 200	23 800	19 900	21 400
0.6081	15 300	21 300	22 500	19 900	25 000
0.5502	12 500	20 100	21 100	17 000	23 100
0.4979	13 900	18 800	19 700	13 700	22 300
0.4505	14 700	17 700	14 000	14 700	20 400
0.4076	16 600	16 800	11 900	16 200	24 300
0.3688	16 900	16 300	11 100	14 600	17 600
0.3337	9 740	15 300	10 400	14 800	14 400
0.3020	8 960	14 300	9 640	15 900	16 300
0.2752	7 980	13 300	8 970	15 700	17 800
0.2472	7 900	12 400	8 300	12 200	11 000
0.2237	7 720	11 600	7 700	13 400	11 800
0.2024	7 200	10 900	7 100	7 960	17 400
0.1832	9 580	10 200	6 570	12 300	12 000
0.1657	6 980	9 450	6 090	12 900	14 200
0.1500	6 460	8 690	5 650	12 800	23 400
0.1357	8 890	7 940	5 230	7 900	17 300

TABLE I—(*Continued*).

	barn – eV				
Lower Neutron Energy, MeV	Type 316 Stainless Steel	Mo	Cb	V	Al
0.1228	6 430	7 220	4 860	9 610	5 300
0.1111	3 590	6 520	4 510	12 700	7 300
0.08652	5 120	5 540	3 970	4 290	12 300
0.06738	5 880	4 360	3 190	7 040	5 800
0.05247	2 980	3 420	2 540	8 980	1 700
0.04087	2 840	2 700	2 030	3 022	2 600
0.03183	2 680	2 140	1 640	2 650	8 800
0.02479	7 600	942	1 310	3 620	9 700
0.01930	714	1 700	1 030	8 900	3 800
0.01503	1 200	1 350	836	11 300	4 400
0.01171	1 160	1 070	667	10 200	4 400
eV					
9119	756	838	546	2 710	3 400
7102	1 260	653	473	9 440	2 800
5531	810	513	383	5 860	4 200
4307	617	403	306	838	1 800
3355	452	318	245	676	1 400
2613	288	249	198	239	1 100
2035	203	231	160	141	840
1585	117	191	131	102	650
1234	127	160	109	60.8	500
961.1	230	136	91.1	34.9	380
748.5	78.4	120	77.6	19.1	290
582.9	63.2	134	73.3	10.3	220
457.3	48.1	107	79.4	10.2	160
353.6	5.03	118	79.4	12.3	120
275.4	5.07	91.0	79.4	14.9	85
214.5	5.70	51.2	79.4	6.58	59
167.0	6.35	66.0	79.4	10.9	38
130.1	7.17	144	79.4	25.4	23
101.3	8.10	126	79.4	21.3	13
78.89	9.10	94.0	79.4	10.1	15
61.44	10.2	190	79.4	11.1	21
47.65	11.54	584	79.4	12.9	25
37.27	13.1	945	79.4	14.4	29
29.02	14.8	184	79.4	16.8	32
22.60	16.8	26.2	79.4	19.4	26
17.60	19.1	12.4	46.5	21.5	35
13.71	21.6	19.1	2.50	24.2	37
10.68	24.6	39.3	2.83	27.4	38
8.315	27.6	20.8	3.22	31.2	44
6.476	31.2	12.3	3.64	35.2	62
5.043	35.3	11.8	4.13	39.9	77
3.928	40.0	12.5	4.67	45.2	89
3.059	45.4	13.9	5.29	50.8	98
2.382	51.3	14.7	5.99	58.0	110

TABLE 1—(*Continued*).

	barn – eV				
Lower Neutron Energy, MeV	Type 316 Stainless Steel	Mo	Cb	V	Al
1.855	58.2	16.6	6.81	65.7	110
1.445	66.8	18.8	7.69	74.5	110
1.125	76.3	21.3	8.73	84.4	120
0.8764	84.4	24.2	9.91	95.6	130
0.6826	95.0	27.4	11.2	108	190
0.5316	108	31.0	12.7	123	240
0.4140	122	35.2	14.4	158	280
0.0220	212	61.0	24.9	273	390

[a] Function is $E_d^{th} \times F(E)$. To obtain dpa per n/cm², multiply by $1/(E_{d\ \text{preferred}} \times 10^{-24}$. For these calculations $0.6 \times 10^{-24}/E_d^{th}$ is used.

[b] Upper neutron energy is 14.9 MeV.

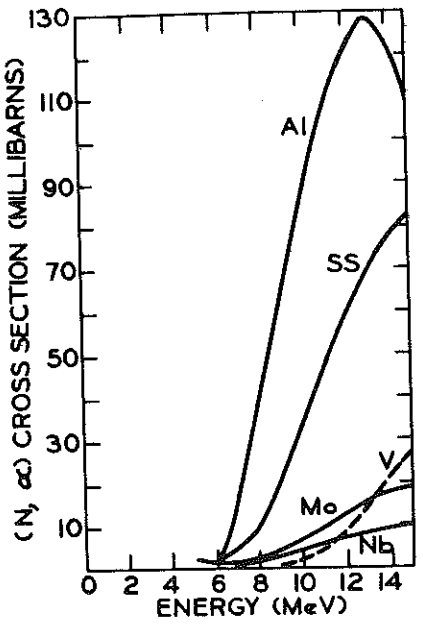

FIG. 1—*Comparison of threshold* (N, ∝) *cross sections for Type 316 stainless steel, vanadium, columbium, molybdenum and aluminum.*

but the calculated results reported later will include those contributions for SAP. The $(n,n'p)$ cross sections will also be included for nickel and chromium as well as the $(n,n'p)$, (n,d), and (n,t) cross sections in SAP.

Results

Displacement Rates

The calculated results for the five materials in the seven nuclear facilities considered here are given in Table 2. The displacement rates in the first wall of a fusion system vary from a low of 2.3×10^{-7} displacements per atom (dpa)/s to 5.4×10^{-7} dpa/s in aluminum. In all cases considered here, the fission reactors had higher displacement rates by a factor of 1.4 to 9.2. The two accelerator neutron sources considered have lower displacement rates than the first wall of the fusion blanket, LAMPF by a factor of ~3.4 and RTNS by a factor of 22. This latter number will always be a constant factor of 22 below the fusion reactor numbers because of our previous assumption about the use of blankets on RTNS.

A comparison of the values in Table 2 to the variation of the damage in the CTR blanket composed of Type 316 stainless steel is shown in Fig. 2. It is noted again that, in general, the fission reactors can produce dpa rates greater than those found in a CTR blanket at a 1 MW/m^2 wall loading. On the other hand, the LAMPF and RTNS facilities can duplicate the CTR displacement rates in only parts of the blanket that are $> \sim 40$ cm or so from a moderately irradiated CTR first wall. The above remarks generally apply as well to the molybdenum, columbium, vanadium, and SAP systems.

Gas Production

The rate of helium and hydrogen generation in the materials of interest is listed in Table 3. Unlike the displacement calculations, there are dramatic

TABLE 2—*Calculated maximum displacement rates for typical nuclear facilities.*

	dpa/s $\times 10^7$				
Facility	Type 316 Stainless Steel	Cb	Mo	V	Al
Fusion Reactor (1 MW/m^2)	3.1	2.3	2.6	3.7	5.4
FFTF (400 MW)	26	16	19	34	49
EBR-II (62.5 MW)	14	9.0	9.6	17	24
HFIR (100 MW)	14	7.8	8.4	16	19
ETR (175 MW)	5.1	3.2	3.5	6.6	8.4
RTNS (2×10^{12}n/cm^{-2}/s^{-1}, 14 MeV)	0.14	0.10	0.12	0.12	0.24
LAMPF (2×10^{14}n/cm^{-2}/s^{-1}, total)	0.84	0.6	0.6	1.1	1.4

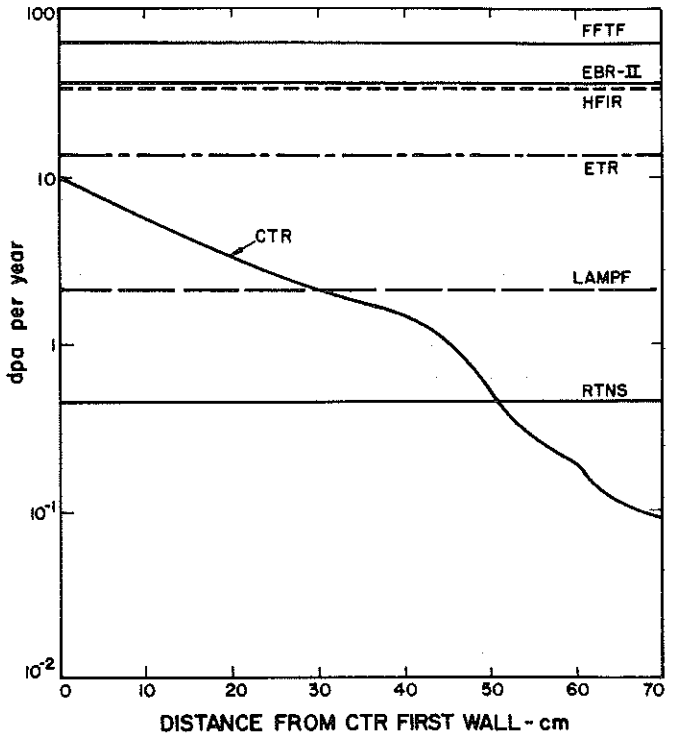

FIG. 2—*Displacement rate in Type 316 stainless steel for various nuclear facilities assuming a 100 percent plant factor.*

differences between the gas production rates of the various materials in the same reactors. For example, the total helium production rate of SAP in the fusion system is twice that of Type 316 stainless steel, over 7 times that in vanadium and molybdenum and over 17 times that for columbium. A slightly different circumstance exists in fission facilities (for example, HFIR) where the ^{59}Ni reactions cause over 100 times more helium to be formed in Type 316 stainless steel than SAP. It is best at this point to discuss the results in terms of a specific gas in an individual material.

The calculated helium production in Type 316 stainless steel ranges from a low of 1.5×10^{-7} appm/s in EBR-II to 1330×10^{-7} appm/s after one year of irradiation in HFIR. The ETR facility produces close to the same amount of helium as does a fusion spectrum although the reactions in the two systems are completely different. In the thermal fission reactors (HFIR and ETR), most of the helium comes from the ^{59}Ni reaction whereas in the fast reactors most of the helium comes from primary reactions. It is important to remember that the "rate" of helium production is not constant in thermal fission reactors; it starts out constant and increases as $(\phi t)^2$ until such time as burn out in ^{59}Ni becomes important. Thereafter, the production rate drops until it is eventually proportional to t to the first power. The

TABLE 3—*Calculated gas production rates for typical nuclear facilities.*

Facility	appm/s × 10^7					
	Type 316 Stainless Steel[a]	Type 316 Stainless Steel[b]	Cb	Mo	V	SAP
	Helium					
CTR	64	N[c]	7.6	15	18	130
FFTF	2.5	N	0.53	0.95	0.15	5.5
EBR-II	1.5	N	0.31	0.57	0.097	2.5
HFIR	2.6	1330	0.57	1.0	0.15	5.8
ETR	0.61	48	0.15	0.27	0.030	1.3
RTNS	2.9	N	0.34	0.68	0.81	5.9
LAMPF	5.1	N	0.62	1.2	1.3	9.1
	Hydrogen Isotopes					
CTR	170		25	30	33	250
FFTF	133		3.6	1.8	7.7	33
EBR-II	85		2.1	1.1	4.6	16
HFIR	141		3.9	1.9	8.5	36
ETR	43		1.1	0.53	2.5	11
RTNS	7.7		1.1	1.4	1.5	11
LAMPF	19		2.23	2.5	2.8	19

[a] Primary reactions only.
[b] Helium (appm/s × 10^7) contribution from $^{58}Ni(n,\gamma)^{59}Ni(n,\alpha)$ after only one year of irradiation.
[c] N = negligible, $<<0.1 \times 10^{-7}$appm/s^{-1}.

data in Table 3 is reported as the instantaneous rate from both helium threshold reactions and $^{59}Ni(n,\alpha)^{55}Fe$ reactions after one year of continuous operation.

Figure 3 shows an example of how the helium generation rates vary throughout a Type 316 stainless steel CTR blanket. A comparison is also made to helium production in other facilities. It is noted that fast fission and accelerator sources considerably underproduce helium, by a factor of 10 or more, in steel compared to that in the first wall of a 1 MW/m^2 neutron irradiated CTR first wall. In fact, the nonfusion sources cannot generate enough helium to duplicate the production rates in the first 40 to 50 cm of such a blanket. On the other hand, thermal reactors may duplicate the helium production rates up to ~7 MW/m^2.

The vanadium system has no thermal (n,α) reaction and, therefore, the amount of helium produced by the neutron facilities is only from primary

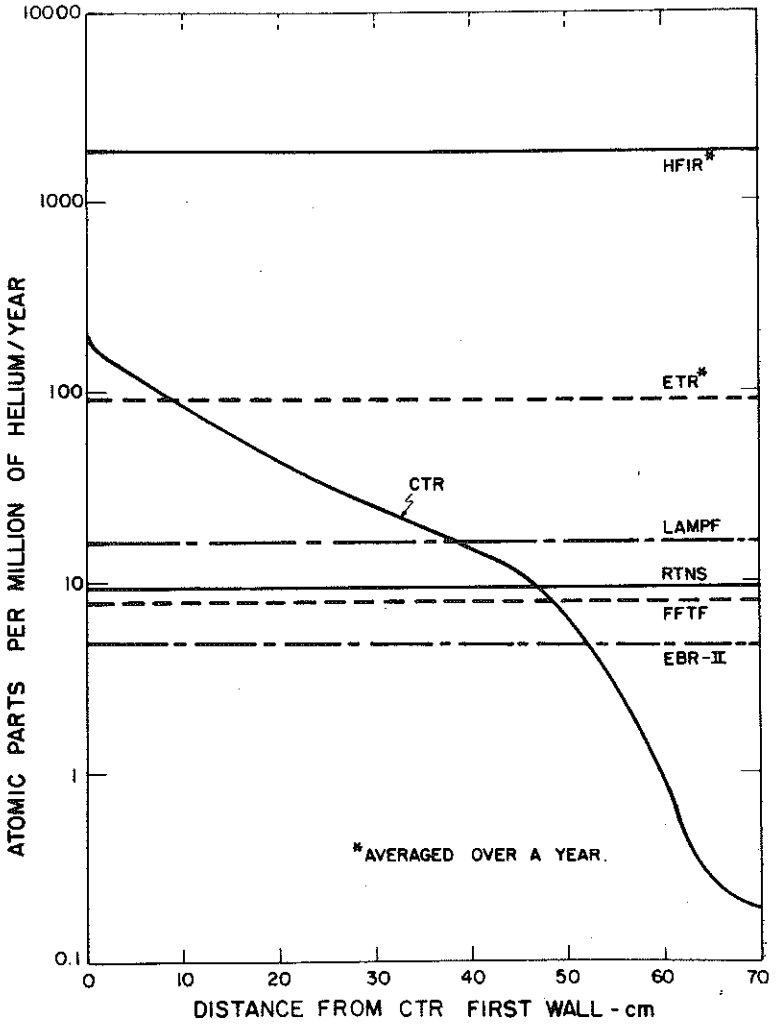

FIG. 3—*Calculated helium production rate in Type 316 stainless steel for various nuclear facilities.*

reactions. The production rate in the CTR blanket is at least two orders of magnitude larger than that in fission reactors. It is interesting to note that the RTNS can produce helium at a rate 10 times that in the EBR-II and the helium production rate in the LAMPF facility is ~60 percent higher than that in the RTNS.

Columbium has the lowest helium production rate of any of the five materials considered here. However, the maximum value of 7.6×10^{-7} appm/s^{-1} in the fusion system is still more than a factor of 10 higher than for the best fission facilities. Another interesting point in this metal is that the accelerator sources can produce helium in columbium at about the same rate as do the EBR-II and FFTF reactors.

The situation for molybdenum is slightly different than that of vanadium

in that fission facilities, and accelerator sources produce helium at a rate which is only one order of magnitude lower than in a fusion reactor.

The SAP alloy has the highest helium generation rates of any material considered here except for the steel in thermal fission reactors. About 10 percent of this high helium generation rate in the fusion reactor stems from the fact that the $(n,n'\alpha)$ reaction has been included in this calculation. About 20 percent of the helium in SAP comes from (n,α) and $(n,n'\alpha)$ reactions in the oxygen of the aluminum oxide. However, even if the contribution from oxygen is subtracted, pure aluminum alone still produces more gas than any of the other materials considered here.

The major difference between the hydrogen isotope and helium production in Type 316 stainless steel is that there is no thermal (n,p) cross section in steel and about 60 percent of the hydrogen in steel comes from nickel which is present as ~14 atomic percent. The hydrogen isotope production rates in SAP include a contribution from the aluminum $(n,n'p)$ cross section of 12 percent and as 18 percent donation from the (n,d) reaction. Finally, it should be noted that while oxygen contributes ~20 percent of the helium to SAP, it only contributes 1 percent of the hydrogen isotopes.

Discussion

There are four main features of this work which deserve special discussion.

1. There is similarity in the energy dependencies of the displacement cross sections for all the materials studied here.

2. The displacement rates in all parts of CTR blankets at moderate wall loading (~1 MW/m^2) are below those in current fission reactor research facilities (Fig. 2).

3. There are extremely high helium production rates for all materials in CTR and for Type 316 stainless steel in thermal reactors (Table 3 and Figs. 3 and 4).

4. A large discrepancy exists between helium production rates in CTR as opposed to most other research facilities (Table 3 and Fig. 3).

The relative magnitudes of the displacement cross sections are uncertain to perhaps 30 percent. This is of minor importance in this work, however, because absolute comparisons of displacement rates of several materials in a given irradiation facility provide little or no information on comparative "total damage rates." This is because of the extreme sensitivity of radiation damage to such variables as material purity and microstructure. Legitimate comparisons among materials of the spectrum dependence of the displacement rate can be made by first normalization all displacement rates in one spectrum to unity. When this is done, it is found that relative rates differ by $< \pm 25$ percent (generally considerably less). Hence, any

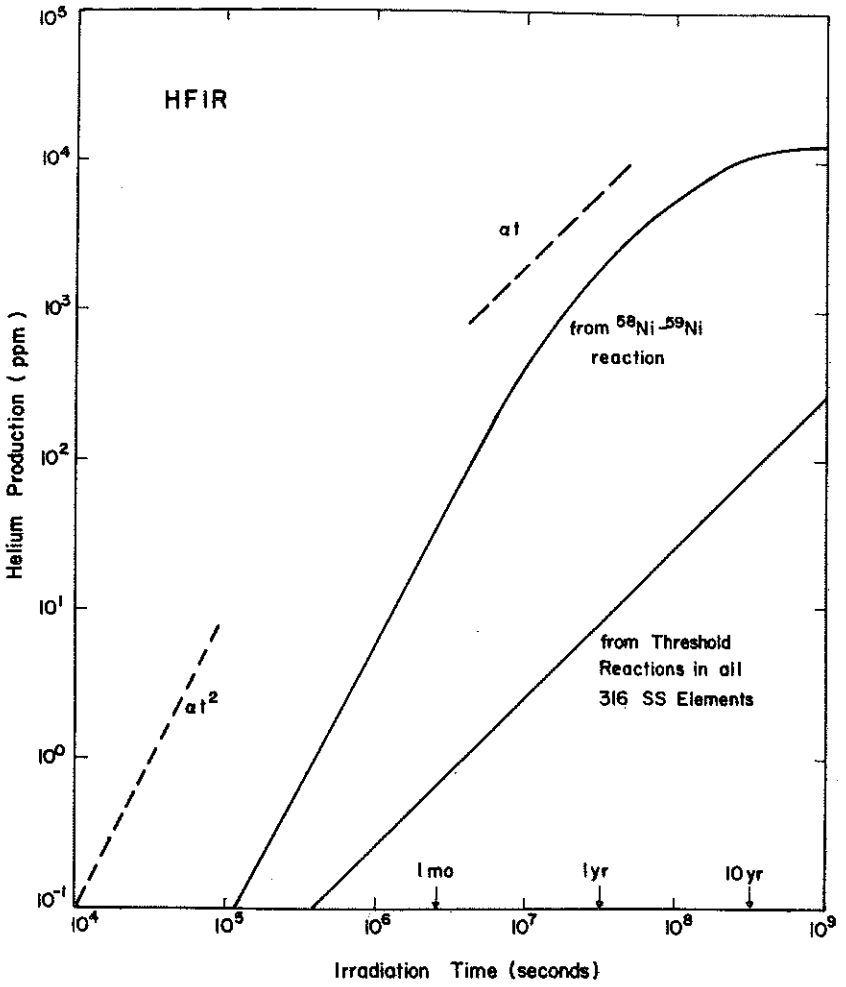

FIG. 4—*Helium gas production in Type 316 stainless steel.*

conclusions made regarding the simulation of CTR displacement rates with fission reactors applies to all five of the materials studied.

It is interesting to note that even though we have calculated the displacement rate of solid members in a 4000 MW(th) CTR, these rates are substantially below those which could be produced in lower power fission plants. This effect is mainly due to the size of CTR and the substantial separation of the solid blanket members from the neutron generating media, (the plasma) in fusion systems. Figure 2 shows that, provided the wall loading of fusion systems does not exceed a few MW/m^2, all of the four fission reactors considered here can produce damage rates higher than in the CTR first wall. The FFTF can even duplicate displacement damage typical of ~7 to 9 MW/m^2 neutron wall loading.

An important point to note in Figs. 2 and 3 is the fact that the total damage in the blanket could vary by more than two orders of magnitude. The

variation in total damage for components which extend radially from the CTR first wall would introduce rather severe complications. Differential swelling, hardening, or creep could cause local bending or warping of structural components and introduce unacceptable stresses. Not only could the total damage vary significantly but the damage rate could vary from as little as 3×10^{-9} dpa/s^{-1} at the outer edge of the blanket to $\sim 3 \times 10^{-7}$ dpa/s^{-1} at the first wall of a 1 MW/m^2 loaded system. Future irradiation programs will have to take both of these effects into account because recent evidence [*33*] has shown than at relatively moderate temperatures (30 to 50 percent of the melting point) the rate at which damage is induced may affect the final configuration of defects. It is also well known that such processes as creep, a higher temperature phenomenon, are also very sensitive to damage rate [*34*].

Unlike the displacement results which are relatively insensitive to the material, the production of helium or hydrogen in potential CTR materials depends very much on the elements considered. For example, it can be seen that in the first wall of a CTR blanket the helium production rate in SAP is 7 to 17 times that of refractory metals while the displacement rates of these metals are within 25 percent. The hydrogen production rate in the SAP is also 4 to 5 times higher than for refractory metals. Because of the various threshold energies, the ratios are even more pronounced in fast fission facilities. Another good example is the helium production in steel in fast reactors. It occurs at a rate 5 times higher in Type 316 stainless steel than in columbium and almost 3 times higher than in molybdenum. Hydrogen production in steel is 17 times higher than in vanadium and 37 times higher than in columbium for fast reactors. On the other hand, thermal reactors like HFIR can produce helium in steel more than 20 times faster than in fusion reactors if enough time is given for a buildup of ^{59}Ni. The buildup of helium in Type 316 stainless steel irradiated in HFIR is shown in Fig. 4. Initially ($\sim <$ 1 month) the helium production rate due to ^{59}Ni (n,α) reactions is proportional to t^2. After a few months, the production rate is proportional to the first power of time because the ^{59}Ni (n,γ) reaction begins to compete. Finally, when all of the ^{58}Ni atoms have been transmutted, there is no more helium produced by this type of reaction and only the high energy (n,α) reactions can contribute more helium. This complex behavior tends to emphasize the point that when scientists study irradiation induced phenomena which may be affected by gas atoms (for example, voids and ductility reductions), they must analyze the neutron spectra very carefully.

Variations of gas production in different structural materials has certainly been expected by investigators. However, variations in gas production in the same material irradiated in different neutron spectra can also be important. Figure 3 shows that the absolute helium production rates

in neutron test facilities could vary in stainless steel by two to three orders of magnitude. This is particularly important because the CTR blanket design considered here has a relatively low neutron wall loading (1 MW/m^2), and other systems have been designed to as high as 6 MW/m^2 [35]. It is obvious from Fig. 3 that even the FFTF, the highest flux fast reactor in the United States, cannot duplicate much more than a 0.04 MW/m^2 wall loading from the standpoint of helium gas production; but the ETR can duplicate a 0.75 MW/m^2 value, and HFIR can duplicate the helium production rate of ~7 MW/m^2 wall loading. The high energy neutron facilities are within an order of magnitude of reasonable CTR gas generation.

The situation is somewhat worse for the refractory metals such as vanadium where wall loadings of only ~0.01 MW/m^2 can be duplicated in FFTF and HFIR for the production of helium. The accelerator sources can duplicate helium production rates of only 0.05 MW/m^2. The same conclusion applies to the other CTR metals and it is clear that no "existing" facility can duplicate the proper CTR gas production rates for columbium, vanadium, molybdenum, or SAP.

The previous points can be put into a little better perspective by calculating the ratio of the gas production to the displacement rates. The results for the helium to dpa ratio are shown in Fig. 5, and specific values can be obtained by dividing the numbers in Table 3 by those in Table 2. It is important to note that this ratio is *not* dependent on absolute flux values (with the exception of Type 316 stainless steel) but depends only on energy spectra. Whereas, the atomic parts per million helium/dpa ratio in steel is ~20 in the CTR first wall, it is only 0.10 to 0.14 in fast fission reactors, but ~50 in HFIR after one year of irradiation. This ratio drops to ~6 in LAMPF. The ratio for vanadium varies by ~3 orders of magnitude from CTR to fast fission plants, and it varies by ~2 orders of magnitude for SAP and molybdenum in the same facilities. The high energy accelerator neutron facilities tend to have better ratios for the nonsteel materials but they are still a factor of three or more lower than typical CTR values. Hence, any experiments done on non-CTR facilities which purport to correlate with CTR conditions must be closely examined in view of the helium/dpa ratio.

The situation with respect to the hydrogen/dpa ratio is much the same as for the helium ratio. This ratio varies by a factor of ~10 for steel when comparing such facilities as FFTF and the first wall of a CTR. There is also a one to two order of magnitude difference in the hydrogen/dpa ratio for columbium the same facilities.

One final point to notice from Figs. 2 to 5 is that the HFIR reactor

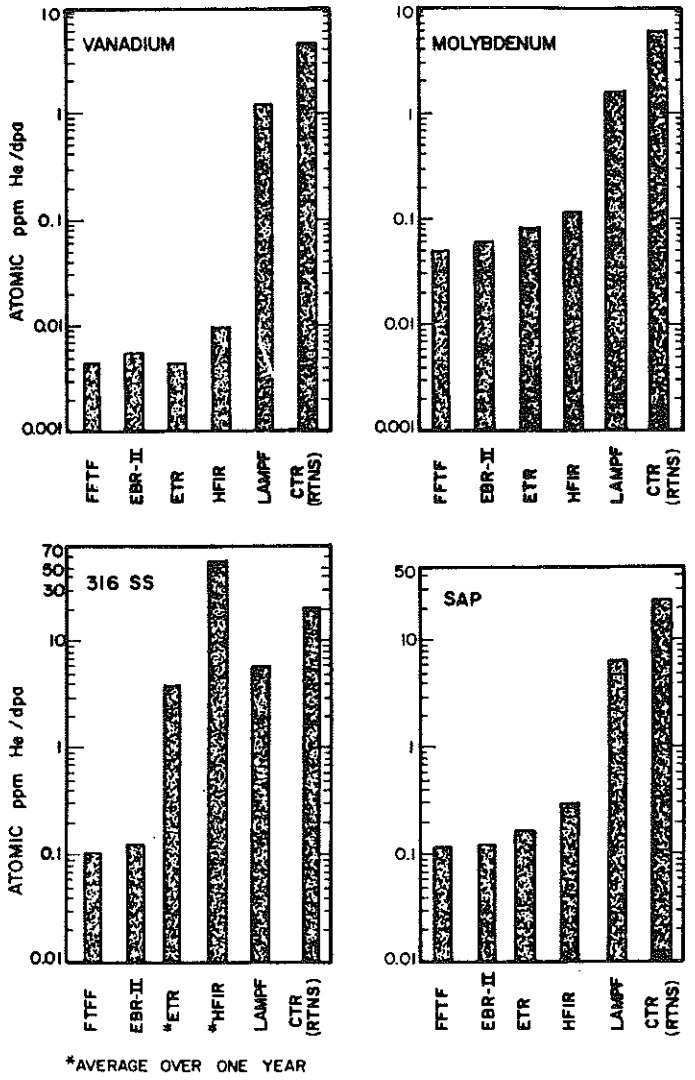

FIG. 5—*Calculated helium to displacement ratio in various nuclear facilities.*

represents perhaps the best combination of dpa rates, helium/dpa and hydrogen/dpa ratios for the materials considered here. The high flux FFTF has adequate dpa rates but hydrogen/dpa and helium/dpa ratios that are quite low. Accelerator neutron sources produce close to the proper gas displacement ratios but the absolute magnitude of the damage rate is so low that it could take ~10 years of irradiation to reproduce ~one year of CTR first wall damage due to gas effects. Improvement in these facilities by a factor of ten would make them much more attractive as irradiation test facilities.

Conclusions

1. The variation of the spectrum averaged displacement cross section among existing irradiation facilities is the same, to within ±25 percent, for columbium, molybdenum, vanadium, aluminum, and Type 316 stainless steel.

2. There will be large variations in the rate at which atoms are displaced in a standard CTR blanket, up to a factor of 100 in this study.

3. Several present neutron facilities can duplicate displacement rates in CTR blankets with ~ 2 to 8 MW/m^2 neutron wall loadings.

4. The relative helium production rates in the first wall of a CTR blanket will vary in the following proportion for SAP, Type 316 stainless steel, vanadium, molybdenum, or columbium, 17/8.4/2.4/2/1. Similar numbers for hydrogen generation vary in the ratio of 10/6.8/1.3/1.2/1.

5. The helium production rates in the first wall of a CTR in appm/year/MW/m^{-2} wall loading are 410/202/57/47/24 for SAP, Type 316 stainless steel, vanadium, molybdenum, and columbium, respectively. Similar numbers for hydrogen are 790/540/100/95/79.

6. The variation in helium production rates from the first wall of a standard CTR to the outer edge of the blanket is ~1000.

7. While there are large variations from element to element, it is clear that fast fission reactors will produce atomic parts per million helium/dpa ratios which are a factor of ~100 or lower than that produced in the first wall of CTR blankets.

8. The helium production rates in Type 316 stainless steel in thermal fission reactors can be even higher than in fusion reactor blankets due to the buildup of ^{59}Ni and the subsequent (n,α) reactions. Helium production rates of several thousand atomic parts per million per year can be achieved in high flux thermal reactors like HFIR.

9. All current fission reactors will produce an atomic parts per million hydrogen/dpa ratio of 5 to 100 times lower than that found in the first wall of CTR blankets.

10. High energy neutron sources such as the RTNS and LAMPF facility can produce gas/dpa ratios close to or within a factor of 4, those found in CTR blankets. However, the absolute magnitude of gas production is lower by a factor of 10 or more.

11. The thermal reactor HFIR appears to have the best combination of displacement and gas production rates and gas/displacement ratios with which to conduct present CTR materials studies, especially for stainless steel.

Acknowledgments

The authors would like to thank the Wisconsin Electric Utilities Research Foundation and the U.S. Atomic Energy Commission Controlled Thermonuclear Research Division and Reactor Research and Development Division for their support of this work. We would also like to thank Donald Dudziak for allowing us to use LAMPF spectra.

References

[1] "Nuclear Fusion Reactors," *Proceedings*, J. L. Hall and J. H. C. Maple, Eds., British Nuclear Energy Society Conference, Culham Laboratory, England, Sept. 1969.

[2] Steiner, D., *Nuclear Applications and Technology*, Vol. 9, 1970, p. 83.

[3] *Proceedings*, International Working Sessions on Fusion Reactor Technology, D. Steiner, Ed., CONF-710624, Oak Ridge, Tenn., 28 June 1971.

[4] *Proceedings*, Meeting on Fusion Reactor First Wall Materials, L. C. Ianniello, Ed., WASH-1206, U. S. Atomic Energy Commission, Jan. 1972.

[5] Kulcinski, G. L., Brown, R. G., Lott, R. G., and Sanger, P. A., *Nuclear Technology*, Vol. 22, 1974, p. 11.

[6] *Radiation Induced Voids in Metals*, J. W. Corbett and L. C. Ianniello, Eds., U. S. Atomic Energy Commission, June 1971.

[7] "Voids Formed by Irradiation of Reactor Materials," British Nuclear Energy Society, Reading, England, 1971.

[8] *Effects of Radiation on Substructure and Mechanical Properties of Metals and Alloys, ASTM STP 529*, American Society for Testing and Materials, 1973.

[9] Holmes, J. J., Lovell, A. J., and Fish, R. L. in *Effects of Radiation on Substructure and Mechanical Properties of Metals and Alloys, ASTM STP 529*, American Society for Testing and Materials, 1973, p. 383.

[10] Bloom, E. E. in *Irradiation Embrittlement and Creep in Fuel Cladding and Core Components*, British Nuclear Energy Society, London, 1973.

[11] Kramer, D., Garr, K. R., Pard, A. G., and Rhodes, C. G. in *Irradiation Embrittlement and Creep in Fuel Cladding and Core Components*, British Nuclear Energy Society, London, 1973.

[12] Hirsch, R. L., *Proceedings*, 1972 International Conference on Nuclear Solutions to World Energy Problems, American Nuclear Society, Hilsdale, Ill., 1973, p. 216.

[13] Badger, B., Abdou, M. A., Boom, R. W., Brown, R. G., Cheng, T.E., Conn, R. W., Donhowe, J. M., El-Guebaly, L. A., Emmert, G. A., Hopkins, G. R., Houlberg, W. A., Johnson, A. B., Kamperschroer, J. H., Klein, D., Kulcinski, G. L., Lott, R. G., McAlees, D. G., Maynard, C. W., Mense, A. T., Neil, G. R., Norman, E., Sanger, P. A., Stewart, W. E., Sung, T., Sviatoslavsky, I., Sze, D. K., Vogelsang, W. F., Wittenberg, L., Yang, T. F., and Young, W. D., *Wisconsin Tokamak Reactor Design*, Vol. 1, UWFDM-68, University of Wisconsin, Madison, Wis., Nov. 1973.

[14] Engle, W. W., "A Users Manual for ANISN—A One Dimensional Discrete Ordinated Transport Code with Anisotropic Scattering," USAEC Report K-1693, U. S. Atomic Energy Commission, Washington, D. C., 1967.

[15] *Data Formats and Procedures for the ENDF Neutron Cross Section Library*, M. K. Drake, Ed., BNL-50279, Brookhaven National Laboratory, Oct. 1970.

[16] Abdou, M. A., Maynard, C. W., and Wright, R. Q., "MACK—A Program to Calculate Neutron Energy Release Parameters and Multigroup Cross Sections From ENDF/B," ORNL-TM-3994, Oak Ridge National Laboratory, Oak Ridge, Tenn., 1973.

[17] Powell, J. R., Miles, F. T., Aronson, A., and Winsche, W. E., "Studies of Fusion Reactor Blankets with Minimum Radioactive Inventory and Tritium Breeding in Solid Lithium Compounds," BNL-18236, Brookhaven National Laboratory, June 1973.

[18] Kam, F. B. K. and Swanke, J. H., "Neutron Flux Spectrum in the HFIR Target Region," ORNL-TM-3322, Oak Ridge National Laboratory, Oak Ridge, Tenn., March 1971.
[19] Dudziak, D. J. and Sherman, M. A., "Neutron Flux Spectra at LAMPF for CTR Radiation Damage Studies," LA-DC-72-1364, Los Alamos Laboratory, Los Alamos, N. Mex., 1972 and unpublished results.
[20] Booth, R. and Barschall, H. H., *Nuclear Instruments and Methods,* Vol. 99, 1972, p. 1.
[21] Lindhard, J., Nielsen, V., Schraff, M., and Thomsen, P. V., *Matematisk-fysiske Meddelelser Danske Videnskabernes Selskab,* Vol. 33, No. 10, 1963.
[22] Robinson, M. T., *Proceedings,* British Nuclear Energy Society Conference, Culham Laboratory, Sept. 1969, p. 364.
[23] Doran, D. G., Beeler, J. R., Dudey, N. D., and Fluss, M. J., "Report of the Working Group on Displacement Models and Procedures for Damage Calculations," HEDL-TME-73-76, Hanford Engineering Development Laboratory, Richland, Wash., Dec. 1973.
[24] Youngblood, G., Myhara, S., and DeFord, J. W., Coo-1494-7, 1968.
[25] Lucasson, P. G. and Walker, R. M., *Physical Review,* Vol. 127, 1962, p. 485.
[26] Neeley, H. M. and Bauer, W., *Physical Review,* Vol. 149, 1966, p. 535.
[27] Doran, D. G., *Nuclear Science and Engineering,* Vol. 49, 1972, p. 130.
[28] Orphan, V. J., Rasmussen, N. C., and Harper, T. L., "Lime and Continuum Gamma Ray Yields from Thermal-Neutron Capture in 75 Elements," GA-10248, Gulf Atomic Report, La Jolla, Calif., July 1970.
[29] Kulcinski, G. L., Doran, D. G., and Abdou, M. A., "Displacement and Gas Production Rates in Candidate CTR Structural Materials," UWFDM-15, University of Wisconsin, Madison, Wis., Feb. 1973.
[30] Segev, M., "Applied Physics Division Annual Report, July 1, 1969—June 30, 1970," ANL-7710, Argonne National Laboratory, Argonne, Ill., Jan. 1971.
[31] Pearlstein, S., *Journal of Nuclear Energy,* Vol. 27, 1973, p. 81.
[32] Kirouac, G., *Nuclear Science and Engineering,* Vol. 46, 1971, p. 427.
[33] Sprague, J. A. and Smidt, F. A., Jr., "Cooperative Radiation Effects Simulation Program," NRL-2629, Naval Research Laboratory, Washington, D. C., Aug. 1973, p. 27.
[34] Harkness, S. D., Yaggee, F. L., and Styles, J. W., "Reactor Development Program Progress Report," ANL-7783, Argonne National Laboratory, Argonne, Ill., Feb. 1971, p. 68.
[35] Thomassen, K. I. and Krakowski, R. A., "A Reference Theta Pinch Experimental Reactor," LA-UR-73-1365, Los Alamos Scientific Laboratory, Los Alamos, N. Mex., Sept. 1973.

DISCUSSION

M. Simnad[1]—What are the prospects for using the "tritium trick" for introducing helium into the materials to simulate helium production in the CTR materials tests?

G. L. Kulcinski, D. G. Doran, and M. A. Abdou (authors' closure)—This technique depends very much on the material considered. For example, it would not work very well for metals that have low hydrogen (tritium)

[1] General Atomics, San Diego, Calif. 92138.

solubility. Secondly, it would not work very well in complex alloys that contain precipitates because of the nonhomogenous distribution of absorbed hydrogen isotopes. The third problem has to do with the injection of all of the helium prior to an irradiation test. Such a procedure is not typical of the constant buildup of helium due to neutronic reactions and may not give the correct result in the final analysis. However, a limited amount of information can be obtained in the vanadium, columbium, and tantalum systems, and such work is now being pursued at Battelle Northwest Laboratory and Lawrence Livermore Laboratory.